UNIVERSITY TURBINE SYSTEMS RESEARCH (UTSR) 2022 GAS TURBINE INDUSTRIAL FELLOWSHIP PROGRAM

Prepared by:

Fynn Reinbacher
Ph.D. Student, Mechanical Engineering
Iowa State University

FINAL REPORT
UTSR Summer 2022 Fellowship

Prepared for:

Southwest Research Institute

September 8, 2022

Benefiting government, industry and the public through innovative science and technology

SOUTHWEST RESEARCH INSTITUTE®
6220 Culebra Road
San Antonio, Texas 78238

University Turbine Systems Research (UTSR) 2022 Gas Turbine Industrial Fellowship Program

Prepared by:
Fynn Reinbacher
Ph.D. Student, Mechanical Engineering
Iowa State University

FINAL REPORT
UTSR Summer 2022 Fellowship

Prepared for:
Southwest Research Institute

September 8, 2022

Approved:

Timothy C. Allison, Ph.D.
Director
Machinery Department

TABLE OF CONTENTS

Section Page

1. INTRODUCTION....1
2. BACKGROUND....2
3. BENCHTOP OXY-FUEL COMBUSTOR....4
   3.1 BACKGROUND....4
   3.2 GOVERNING PARAMETERS....5
   3.3 ORIFICE SIZING....6
      3.3.1 REAL GAS ISENTROPIC FLOW EQUATIONS....6
   3.4 LIGHT-OFF AND START-UP CONDITIONS....7
4. LASER SPARK IGNITION FOR OXY-FUEL COMBUSTION....9
   4.1 EVALUATION OF CURRENT LASER PROBE....9
   4.2 INDEX OF REFRACTION OF REAL GASSES....9
   4.3 GAUSSIAN BEAM PROPAGATION....11
5. SELECTED OTHER PROJECTS AND CONTRIBUTIONS....12
   5.1 FUEL CART UPGRADE FOR NH3 COMPATIBILITY....12
   5.2 MEGAWATT-SCALE OXY-FUEL COMBUSTOR....12
6. ACKNOWLEDGEMENTS....13
7. REFERENCES....14

LIST OF FIGURES

Figure Page

Figure 2-1. Schematic of Allam-Fetvedt cycle. Pure oxygen and natural gas react to release energy, and produce CO_2 and water. Excess water and CO_2 are sequestered from the working fluid. (Fetvedt, 2016)....3

Figure 3-1 Schematic of Benchtop Oxy-Fuel Combustor....4

Figure 4-1. Variation of index of refraction in gases with temperature at elevated pressure 96.5bar (1400psi) (solid), $\pm 2\%$ (dashed), and $\pm 5\%$ (dotted). Blue-carbon dioxide, green oxygen, red methane....10

Figure 4-2. Left: simulated beam waist of collimated Laser beam with wavelength $\boldsymbol{\lambda = 532\ nm}$. Right: schematic of Laser probe. Laser is focused through thin lens with nominal focal length $\boldsymbol{150\ mm}$ through two sapphire windows into supercritical fluid and reflected at concave backwall. The focal location is shifted further away from the lens due to increase index of refraction of fluid....11

1. INTRODUCTION

The U.S. Department of Energy's Office of Fossil Energy and Carbon Management (FECM) strives to reduce the environmental impact of fossil fuels, and move towards global decarbonization in order to meet climate goals. Part of the Advanced Turbine Program managed by the FECM, is the University Turbine System Research (UTSR) Program, which also offers a Gas Turbine Industrial Fellowship (GTIF). The fellowship brings university research students to industrial gas turbine design and manufacturing environments, and engages them in state-of-the-art research and development of advanced turbine systems. Students engage in research in the fields of combustion, aerodynamics/heat transfer, and materials science.

Southwest Research Institute® (SwRI®) facilitates the GTIF program and acts as one of the host companies. This report features work completed as part of the summer fellowship program at SwRI. Highlighted are in particular the evaluation of operating conditions and laser spark ignition of a benchtop oxy-fuel combustor and megawatt scale oxy-fuel combustor for supercritical CO_2 power cycles.

2. BACKGROUND

Transitioning into a carbon neutral energy future requires both the development of renewable and sustainable energy sources, as well as improvements in efficiency and upgrades to conventional power systems. Supercritical CO_2 (sCO_2) based power cycles offer solutions to both endeavors. As a working fluid sCO_2 combines the high density of liquids with the working behavior of a gas. This allows for highly compact and efficient turbomachines and heat exchangers, greatly reducing the footprint of power plants compared to conventional steam-based systems. Additionally, phase transitions between liquid and vapor, and operating conditions in the two-phase regime are avoided all together, eliminating the need to design a system capable of accommodating phase changes. Compared to other alternative working fluids, sCO_2 has the advantages of being chemically and thermally stable, non-toxic, cheap and readily available.

One possible implementation of a sCO_2 power plant is as a direct-fired power cycle. In a direct-fired power cycle fuel and oxidizer are combusted within the working fluid stream (rather than use an external heat source) which heats the working fluid by means of a heat exchanger. Direct-fired oxy-fuel combustion allows for emission free operation. In oxy fuel combustion, fuel such as natural gas, reacts with pure oxygen, leaving CO_2 and water as the sole reaction products. Water can be separated from the working fluid stream and excess CO_2 sequestered at pipeline- and storage-ready conditions. The direct-fired, oxy-fuel, sCO_2 power cycle is called the Allam-Fetvedt cycle (Allam, 2014). A schematic can be seen in Figure 2-1.

Many new engineering challenges need to be addressed to enable widespread implementation of this technology, including but not limited to the development of materials which can reliably handle high-pressure fluids exceeding 100 times atmospheric pressure at elevated temperatures, and achieving stable combustion.

SwRI operates at the forefront of these endeavors by developing and testing key technologies in cooperation with commercial clients, universities, and the Department of Energy. Two such efforts include benchtop and megawatt scale direct-fired test facilities. The 2022 UTSR GTIF program focused on contributing to those efforts in the fields of combustion and thermodynamic analysis.

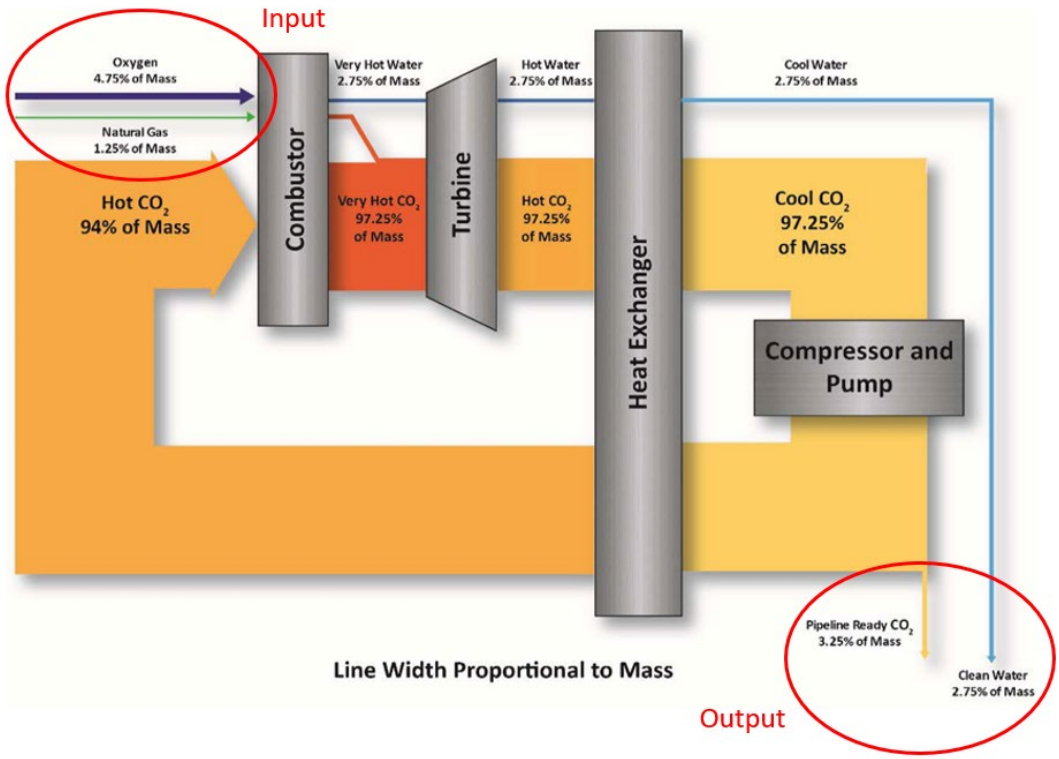

Figure 2-1. Schematic of Allam-Fetvedt cycle. Pure oxygen and natural gas react to release energy, and produce CO_2 and water. Excess water and CO_2 are sequestered from the working fluid. (Fetvedt, 2016)

3. BENCHTOP OXY-FUEL COMBUSTOR

This section provides a summary of SwRI's benchtop oxy-fuel combustor project, and highlights some of the contributions made as part of the UTSR summer fellowship.

3.1 BACKGROUND

While combustion of natural gas in air has been researched extensively, the combustion environment relevant to oxy-fuel combustion in directly fired sCO_2 power cycles currently presents a large knowledge gap in the combustion community. In the literature, typically, high-pressure combustion experiments which investigate flame propagation parameters, cover pressures up to 10bar. At pressures up to 20 or 50 bar the data becomes increasingly sparse. For sCO_2 combustion, typically operating pressures between 100 and 300 bar are targeted. These pressures exceed the critical pressure of carbon dioxide 73.8 bar. Similarly, little data is available for combustion in mixtures with large CO_2 mass fractions, devoid of inert gases such as nitrogen or argon.

The benchtop oxy-fuel combustor at SwRI seeks to facilitate experiments which aid in closing this knowledge gap and serve as a test bed for diagnostic tools for large-scale combustors. Its main components consist of a stainless-steel pressure containment vessel, high-temperature combustion liner, coaxial natural gas burner with CO_2 co-flow, and additional external CO_2 cooling flow. Some of the main challenges in designing this burner include the ignition process, and design of the internal geometry to achieve stable combustion conditions.

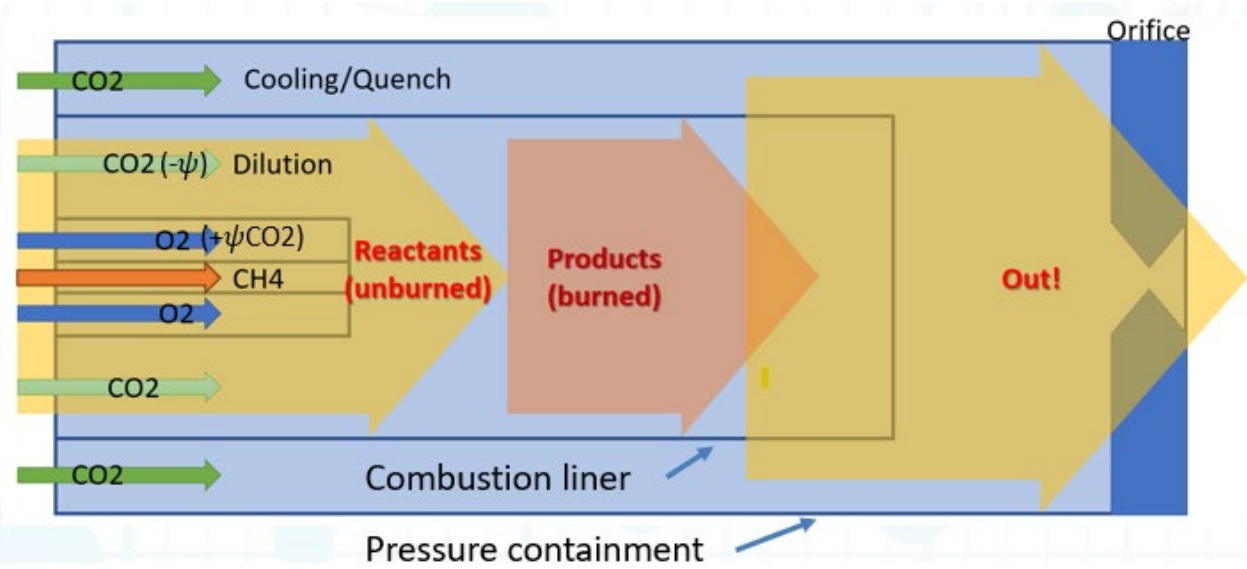

Figure 3-1 Schematic of Benchtop Oxy-Fuel Combustor

The momentum flux ratio (MFR) can be used to estimate mixing between two parallel or coaxial flows. A large MFR causes strong shear forces between the two fluids resulting in turbulence and mixing. The MFR between an inner and an outer flow with mass-flow rates $\dot{m}$ and velocity v can be written as:

$$J_{in/out} = \frac{\dot{m}_{in} v_{in}^2}{\dot{m}_{out} v_{out}^2}.$$

For a given fluid with density ρ through a crosssection A, $\dot{m}$ and v are related via:

$$\dot{m} = \rho v A.$$

A designer can therefore directly target a certain MFR for a given operating condition through their choice of geometry. If J is too small, insufficient mixing will lead to incomplete combustion, if J is too large, excessive strain rates will cause the flame to blowout (Banuti, 2018). To achieve a stable flame, J needs to be just right.

3.2 GOVERNING PARAMETERS

The operation of the Benchtop oxy-fuel rig is largely governed by the chamber pressure p_c, global oxygen mass fraction Y_{O2}, and global equivalence ration ϕ. Temperatures inside the combustor and at the exit are further controlled by the addition of dilution CO_2 and cooling CO_2. Combustion stability and flame holding at the injector are governed by the turbulent mixing of constituents in the shear layers. Velocity and momentum flux ratios of the entering gas streams at the coaxial injector determine the mixing. Once a final geometry is chosen, during testing, operators only have control over a limited number of parameters directly, primarily the mass-flow rates of gas streams entering the combustor. CO_2 from the dilution stream can additionally be blended directly into the oxidizer stream to increase the momentum flux of the oxidizer stream.

An analysis of the sensitivity of the momentum flux ratios between internal dilution/cooling CO_2 in an oxidizer stream and oxidizer and fuel streams was performed. The momentum flux between an inner and outer flow through an annulus is given by:

$$J_{i,o} = \left[\frac{\rho_i v_i^2}{\rho_o v_o^2}\right] = \left[\left(\frac{\dot{m}_i}{\dot{m}_o}\right)^2 \left(\frac{A_o}{A_i}\right)^2 \left(\frac{\rho_o}{\rho_i}\right)\right] = \left[\left(\frac{v_i}{v_o}\right)\left(\frac{m_i}{m_o}\right)\left(\frac{A_o}{A_i}\right)\right].$$

Here the $\dot{m}, \rho, v,$ and A are the respective mass-flow rate, density, velocity and crosssection area of the two flows. If the oxidizer flow gets diluted with a fraction of the dilution CO_2 prior to entering the combustor such that, $\dot{m}_{CO2,cool} = \dot{m}_{CO2}(1-\psi)$ and $\dot{m}_{ox} = \dot{m}_{O2} + \psi\, \dot{m}_{CO2}$, the density of the oxidizer flow can be approximated as:

$$\rho_{mix}(\psi) = \frac{1}{\frac{\dot{m}_{O2}}{M_{O2}} + \frac{\psi\, \dot{m}_{CO2}}{M_{CO2}}}\left[\frac{\rho_{O2}\dot{m}_{O2}}{M_{O2}} + \frac{\rho_{CO2}\, \psi\, \dot{m}_{CO2}}{M_{CO2}}\right].$$

The momentum flux ratios are then given by:

$$J_{f/ox} = c_{f/ox}\left(\frac{\dot{m}_f}{\dot{m}_{O2}}\right)^2 \left(\frac{1}{1+\psi\frac{\dot{m}_{CO2}}{\dot{m}_{O2}}}\right)^2$$

$$J_{ox/cool} = c_{ox/cool}\left[\left(\frac{\dot{m}_{O2}}{\dot{m}_{CO2}}\right)^2 \left(\frac{1}{1-\psi}\right)^2 + \left(\frac{\psi}{1-\psi}\right)^2\right]$$

Where $c_{f/ox}$ and $c_{ox/cool}$ are factors accounting for flow cross section and gas densities.

$$c_{f/ox} = \left(\frac{A_{ox}}{A_f}\right)^2 \frac{\rho_{mix}(\psi)}{\rho_f} \text{ and } c_{ox/cool} = \left(\frac{A_{cool}}{A_{ox}}\right)^2 \frac{\rho_{CO2}}{\rho_{mix}(\psi)}$$

The ratio $\dot{m}_f / \dot{m}_{O2}$ is directly proportional to the equivalence ratio ϕ, and $\dot{m}_{O2} / \dot{m}_{CO2}$ to the global oxygen fraction Y_{O2}.

A number of observations can be made. If mass flow rates inside the combustor are increased or decreased and all other parameters remain fixed, the momentum flux ratios are not impacted as

long as the ratio of the mass flow rates relative to each other remains the constant. The fuel oxidizer momentum flux ratio is primarily impacted by the equivalence ratio. Leaner mixtures will result in lower momentum flux ratios, e.g., less mixing. The global oxygen mass fraction impacts both MFRs. The chamber pressure factors into the momentum flux ratios via the relative changes in density of the individual gases. At low pressures, where gases can be assumed to behave according to the ideal gas equation of state, density ratios will remain constant. At high pressures, real gas effects will take over.

The changes in momentum flux and sensitivities for the Benchtop combustor were further calculated using REFPROP (Lemmon, 2002) real gas properties.

3.3 ORIFICE SIZING

The original design for the Benchtop oxy-fuel combustor sought to employ a back-pressure regulator to elevate the pressure inside the combustion chamber to the necessary operating conditions, at arbitrary mass-flow rates. High temperatures of the exhaust however make the installation of a valve non-trivial. Sealing in most valves is accomplished with seats and seals commonly made from various plastics such as acetal polymers or PTFE. Back-pressure regulation with a valve would, therefore, require additional measures, such as a heat exchanger or quenching with large quantities of high-pressure cool gases, to reduce exhaust temperatures to within the valve's operating limits.

Alternatively, back-pressure generation with a properly sized orifice was investigated. Flow through an orifice or the throat of a converging nozzle is physically limited to reach sonic velocities. This condition is also referred to as choked flow. For a given size orifice and speed of sound of the gas mixture there is a maximum/choked volume flow rate through the orifice. The mass flow rate can then be determined from the volume flow rate and density in the chamber, which is a function of chamber temperature and pressure.

Orifice sizing for the benchtop oxy-fuel combustor was performed using real gas properties using REFPROP (Lemmon, 2002), real gas isentropic flow relations, and chemical kinetics using Cantera (L., 2022) to obtain combustor flame temperatures and equilibrium compositions.

3.3.1 REAL GAS ISENTROPIC FLOW EQUATIONS

At high pressures and temperatures present in highly compressible supercritical gas mixtures, departure from ideal gas behavior can be anticipated. For trans and supercritical fluids the assumptions used to derive isentropic flow relations, which commonly used to calculate the flow conditions through a sonic orifice, start to break down. Real gas effects should, therefore, be accounted for to improve the accuracy of modeling and predictions. An in-depth derivation of real gas isentropic flow relations can readily be found in the literature (Nederstigt, 2017).

One of the primary differences is the introduction of 3 isentropic exponents which factor into each the pressure-temperature isentrope, the pressure-volume isentrope, and the temperature-volume isentrope, γ_{pT}, γ_{pv} and γ_{Tv} respectively. Under ideal gas conditions these reduce back down to $\gamma = \gamma_{pT} = \gamma_{pv} = \gamma_{Tv}$. The real gas isentropic exponents can be calculated as follows:

$$\gamma_{pv} = -\frac{v}{p}\frac{c_p}{c_v}\left(\frac{\partial p}{\partial v}\right)_T,$$

$$\gamma_{Tv} = 1 + \frac{v}{c_v}\left(\frac{\partial p}{\partial T}\right)_v,$$

$$\gamma_{pT} = \left(1 - \frac{p}{c_p}\left(\frac{\partial v}{\partial T}\right)_p\right)^{-1}.$$

They are related by the expression:

$$\frac{\gamma_{pv}}{\gamma_{Tv} - 1} = \frac{\gamma_{pT}}{\gamma_{pT} - 1}.$$

The isentropic relationships retain their familiar form, with the exception of the introduction of the aforementioned real gas exponents:

$$pv^{\gamma_{pv}} = const., \qquad Tv^{\gamma_{Tv}} = const., \qquad Tp^{\frac{1-\gamma_{pT}}{\gamma_{pT}}} = const.$$

Using the real gas isentropic flow relationships, the real gas stagnation conditions can be derived as follows:

$$\frac{p}{p_0} = \left[1 + \frac{\gamma_{pv} - 1}{2} M^2\right]^{-\frac{\gamma_{pv}}{\gamma_{pv}-1}}$$

$$\frac{T}{T_0} = \left[1 + \frac{\gamma_{pv} - 1}{2} M^2\right]^{-\frac{\gamma_{Tv}-1}{\gamma_{pv}-1}}$$

$$\frac{\rho}{\rho_0} = \left[1 + \frac{\gamma_{pv} - 1}{2} M^2\right]^{-\frac{1}{\gamma_{pv}-1}}.$$

The critical area ratio becomes:

$$\frac{A}{A^*} = \frac{1}{M}\left[\frac{2 + (\gamma_{pv} - 1)M^2}{\gamma_{pv} + 1}\right]^{\frac{\gamma_{pv}+1}{2(\gamma_{pv}-1)}},$$

and the critical mass flow rate:

$$\dot{m}^* = A^*\sqrt{\gamma_{pv}\rho_0 p_0}\left(\frac{2}{\gamma_{pv} + 1}\right)^{\frac{\gamma_{pv}+1}{2(\gamma_{pv}-1)}}.$$

These equations allow the calculation of the size of a sonic orifice given a gas flow quantity of known composition, temperature and pressure. Once an orifice size is selected, the variation in chamber pressure for set mass flow rates can be obtained, to simulate a variety of combustor operating points.

3.4 LIGHT-OFF AND START-UP CONDITIONS

Based on the described real gas flow conditions, a set of Python functions and classes was generated to simplify modeling of mixing of various gas streams, account for heat release from chemical reactions, and the variation in mass flow rates. Developed Python classes and functions allow for simplified interfacing between real gas thermodynamic properties and ideal gas chemical reaction models, as well management of properties of multiple gas phases. These tools were employed to aid in the selection of light-off and operating conditions.

Ideally ignition, i.e., light-off, of the combustor would occur at a lower pressure to reduce risk of catastrophic system failures due to sudden additional pressure rises accompanying the heat release. In a system with fixed sonic orifice, mass-flow and chamber pressure are directly related. To enable light-off at a pressure below the target operating condition, mass flow rates need to be reduced, and subsequently slowly increased. During ignition the temperature of the mixture increases, causing the pressure in a constant volume to increase. When selecting operating points all these factors need to be considered, along with the dynamic response and operating limits of gas supply equipment, in particular the control valves.

4. LASER SPARK IGNITION FOR OXY-FUEL COMBUSTION

Compared to conventional ignition methods such as spark or glow plugs, laser spark ignition is less intrusive and requires fewer precautions to create a proper seal. A laser spark is created by focusing a high-power laser pulse into the combustion chamber. At the focal point the intensity of the electric field becomes strong enough to cause the gas to break down and dissociate. The plasma kernel is further heated by the laser causing the mixture to ignite.

4.1 EVALUATION OF CURRENT LASER PROBE

Previous studies at SwRI by Katcher et al. (Katcher, 2019) investigated ignition by laser sparks created pulsed lasers and lenses with short focal lengths in CO_2 at conditions just above the critical point. However, generation of laser sparks with longer focal length in sCO_2 at elevated pressures and subsequent ignition proved difficult. A number of potential issues were identified, including reflective losses due to multiple interfaces, unaccounted changes in index of refraction in supercritical fluids, and backwall reflections.

4.2 INDEX OF REFRACTION OF REAL GASSES

Most laboratory applications using optical operate either in air or a vacuum where the index of refraction is close to 1.0. Optics such as lenses or prisms work based on the difference in index of refraction between the glass or crystal the optic is made of and its surroundings. The index of refraction of a medium is determined by its dielectric constant, the strength of interaction between a single particle and light, its density, and the number of particles interacting with a light wave. The Lorentz-Lorentz equation relates the specific refraction r, index of refraction n, and density ρ to each other.

$$n = \left[\frac{2r\rho + 1}{1 - r\rho}\right]^{1/2}$$

Both index of refraction and specific refraction depend on the wavelength of the light $[r, n] = f(\lambda)$and a gas's density strongly depends on its pressure and temperature, $\rho = f(T, p)$. An equation of state can be used to calculate gas properties. The variation of the index of refraction with wavelength is often given in the form of polynomial such as the Sellmeier equation:

$$n^2 - 1 = \frac{a_1\lambda^2}{\lambda^2 - b_1} + \frac{a_2\lambda^2}{\lambda^2 - b_2} + \frac{a_3\lambda^2}{\lambda^2 - b_3}$$

Here λ is the wavelength and a_i, b_i are parameters for the given material. For gases the index of refraction is often recorded at standard conditions. Using both Sellmeier and Lorentz-Lorentz equation the index of refraction of a gas at elevated pressures and temperatures can be obtained.

Depicted in Figure 4-1 is the variation in index of refraction of methane, oxygen and carbon dioxide at 96.5 bar, dashed and dotted lines represent a pressure variation $\pm 2\%$ and $\pm 5\%$ respectively. It can be seen that at elevated pressures the assumption that gas refractive indices equal 1.0 breaks down. Further a strong dependence of the index of refraction of carbon dioxide on temperature can be observed. Small variations in temperature at super critical conditions can lead to large variations in density and thus index of refraction. For reference, the index of refraction of liquid water at 20°C is ~1.33 and 1.52 for window glass.

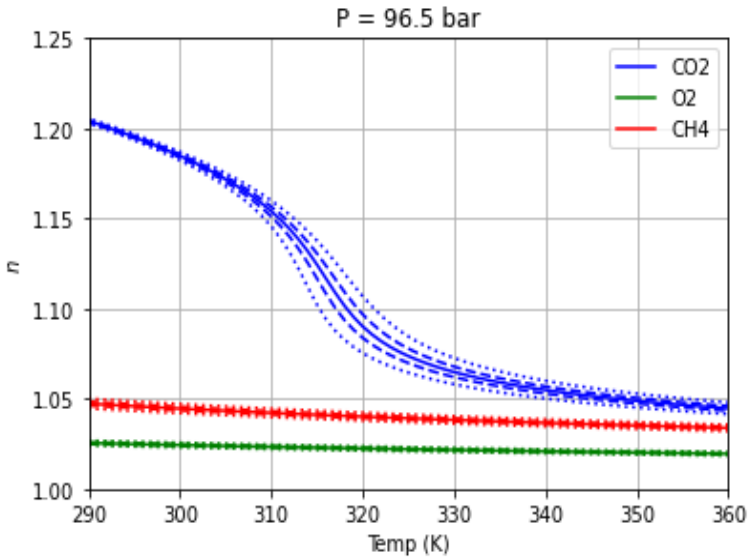

Figure 4-1. Variation of index of refraction in gases with temperature at elevated pressure 96.5bar (1400psi) (solid), $\pm 2\%$ (dashed), and $\pm 5\%$ (dotted). Blue-carbon dioxide, green oxygen, red methane.

An equation for the focal length of a thin lens, focusing light approaching through a medium with index of refraction n_0, a lens made out of a material with index of refraction n_l, and into a medium with index of refraction n_2, can easily be derived. It can be shown that the focal length f_0 determined for focusing in the case where $n_0 = n_2 \approx 1.0$ differs from the focal length f in the case where $n_0 \approx 1, n_2 > 1.0$ by $f \approx n_2 f_0$. In other words, when focusing into supercritical CO_2 the effective focal length of the lens is increased by a factor equal to the index of refraction of the fluid, e.g., for $n(sCO_2) = 1.15$ the focal spot of a lens with 150 mm focal length would instead be located at a distance of 172.5 mm. This does not only impact the necessary alignment and positioning of optics, it also reduces the intensity of the Laser pulse at the focal point.

4.3 GAUSSIAN BEAM PROPAGATION

An ideal laser/electromagnetic wave propagating through space can be described as a Gaussian beam. It does not propagate like a particle or ray in a straight line and cannot be focused to an infinitely narrow spot as ray tracing methods would suggest. The propagation of a Gaussian beam can, however, be modeled using the so-called complex beam parameter, which contains information about the wave front curvature and beam diameter, and Ray Transfer Matrices (RTMs). RTMs mathematically describe the interaction of a Gaussian beam or light ray with an interface, its propagation through free space, or medium with varying index of refraction.

A Python toolkit of functions was implemented to model the propagation of a Gaussian beam through an arbitrary set of interfaces, e.g., windows or lenses, and media, e.g., air, supercritical fluid, and interaction with reflective surfaces. This allows simulation of the beam focusing of a redesigned laser probe and calculation of light intensity at its focus. Shown in Figure 4-2 is the propagation of a light beam through a thin lens, two windows and a supercritical fluid. Finally, it is reflected at a curved metallic backwall. The propagation direction is not reversed in the figure.

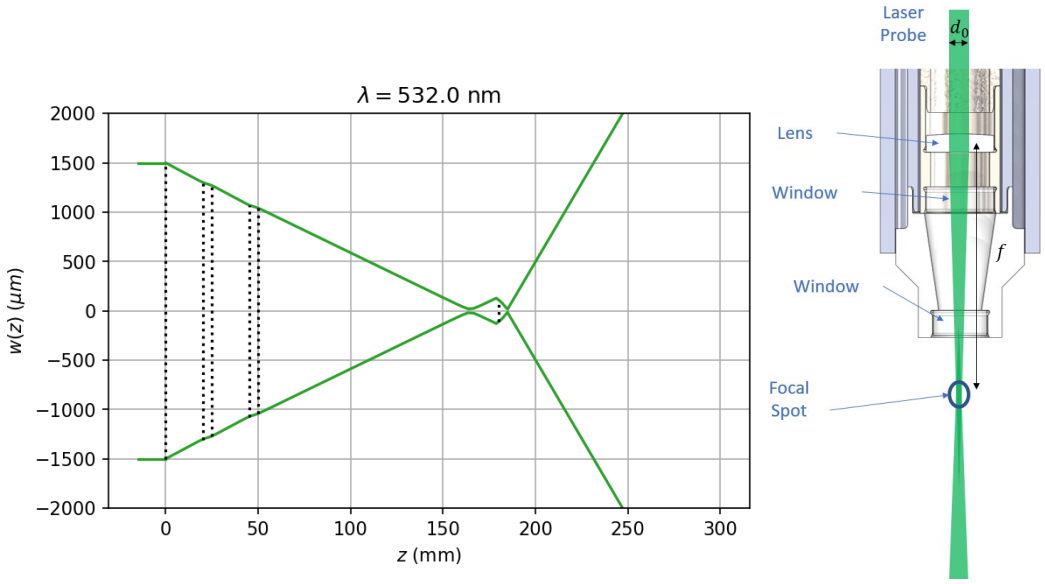

Figure 4-2. Left: simulated beam waist of collimated Laser beam with wavelength $\lambda = 532\ nm$. Right: schematic of Laser probe. Laser is focused through thin lens with nominal focal length $150\ mm$ through two sapphire windows into supercritical fluid and reflected at concave backwall. The focal location is shifted further away from the lens due to increase index of refraction of fluid.

5. SELECTED OTHER PROJECTS AND CONTRIBUTIONS

The UTSR GTIF summer program included participation and contribution to a variety of other, smaller projects, some of which are highlighted here.

5.1 FUEL CART UPGRADE FOR NH3 COMPATIBILITY

An existing fuel cart for supply, flow rate control, and blending of natural gas with hydrogen and inert diluents, such as nitrogen and carbon dioxide, is considered for a future project involving ammonia combustion. Under ideal conditions ammonia reacts with oxygen to form water and nitrogen, thus releasing no greenhouse gases. Due to ammonia's low flame speed, establishing stable combustion conditions is not trivial, encouraging research into blending ammonia with highly flammable fuels such as hydrogen.

Unlike common hydrocarbons, such as methane or propane, anhydrous ammonia is incompatible with many common materials used in flow control instrumentation. In particular many copper alloys such as brass, and many plastics used to create seats and seals in valves are incompatible. In the presence of ammonia, they would foul, corrode, degrade, and cause leaks.

Existing piping and instrumentation (P&ID) were evaluated for material compatibility. Several incompatible valves and seals were identified, along with replacement solutions. The accessible range of gas flow rates by control valves and meters was compared to target flow rates, and appropriate upgrades were identified.

Additionally, the potential need for a designated ammonia vaporization system was evaluated.

5.2 MEGAWATT-SCALE OXY-FUEL COMBUSTOR

A megawatt-scale oxy-fuel combustor is under development at SwRI. Unlike the benchtop combustor, a swirl injector is used to achieve mixing between fuel and oxidizer and stabilize the flame. Similarly, to the benchtop combustor, light-off will need to occur a pressure much lower than the design operating point and a strategy is necessary to establish both light-off conditions and a number of operating points leading up to the final design point.

Contributions were made towards establishing operating ranges considering both operating ranges of piping and instrumentation used to supply and control flows to and from the combustor, and flame holding / burning regimes. Particular focus was on estimating relevant chemical length time scales, compared to length and timescales governing the turbulent swirl flow.

6. ACKNOWLEDGEMENTS

I would like to thank SwRI and the UTSR fellowship program for granting me the opportunity to participate in the GTIF program, funding, and support. Thank you to the SwRI intern program for providing the opportunity to learn about the variety of work performed at the Institute throughout the summer.

I would like to extend a special thank you to my coworkers in the Div. 18 Machinery Department, my mentors and supervisors Griffin Beck, Steve White, and Brian Connelly for their guidance, support, and many great discussions, staff and administration Laura Garcia and Dorothea Martinez for helping me navigate a new workspace, and my fellow division 18 interns for a fun work environment.

7. REFERENCES

Allam, R. a. (2014). The oxy-fuel, supercritical CO_2 Allam Cycle: New cycle developments to produce even lower-cost electricity from fossil fuels without atmospheric emissions. *Turbo Expo: Power for Land, Sea, and Air. 45660*, p. V03BT36A01. American Society of Mechanical Engineers.

Banuti, D. T. (2018). Large eddy simulations of oxy-fuel combustors for direct-fired supercritical CO_2 power cycles. *The 6th International Symposium on Supercritical CO_2 Power Cycles.*

Fetvedt, J. (2016). *Development Of The sCO_2 Allam Cycle.* Supercritical CO_2 Power Cycles Symposium. Retrieved from http://sco2symposium.com/papers2016/Keynote/JeremyFedvet.pdf

Katcher, K. M. (2019). Igniter Testing for sCO_2 Oxy-Combustion. *Turbo Expo: Power for Land, Sea, and Air. 58721*, p. V009T38A017. American Society of Mechanical Engineers.

L., D. G. (2022). Cantera: An Object-oriented Software Toolkit for Chemical. (\url{https://www.cantera.org}, Trans.) doi:10.5281/zenodo.6387882

Lemmon, E. W. (2002). NIST reference fluid thermodynamic and transport properties–REFPROP. *NIST standard reference database, 23*, v7.

Nederstigt, P. (2017). *Real Gas Thermodynamics: and the isentropic behavior of substances.*